Effect of Curved Path Monopulse Radar Platform's Grazing Angle on Height of Floated Targets Detection

FarhadFarnia[1] **MortezaKazerooni**[2]

[1] MSc Graduate, Electrical and computer University Complex, Malek-Ashtar University of Technology
Farhad.farnia@gmail.com

[2] Associate Professor, Electrical and computer University Complex, Malek-Ashtar University of Technology
Kazerooni@mut.ac.ir

Abstract:

Monopulse radarsare one of the most accurate tracking radars used to guide various platforms. Detection and tracking of surface targets with these radars are performed in order to point strike targets. Sea clutter presents challenges for detecting floated targets and in addition to affecting detection height, it can cause errors in monopulse angle finding. In this paper, the airborne monopulse radar with high squint angle has been considered. The radar platform has a curved path. Under conditions of ragged sea, sea clutter has been modeled with k distribution and simulation of return signal from sea surface with big size targets has been performed for the first time. Also, we have analyzed the detection heights in various platforms grazing angles in this paper. The results indicated that by increasing the grazing angle, the height of detecting floated targets decreases due to the increase in the clutter power in comparison with the power of returned signal from targets. Due to the significant changes in the simulation parameters of sea Clutter at the angles i.e. gamma function and Omega parameter, the novelty of this paper is simulation of the sea clutter in range and in high grazing angle (55 to 75 degrees), which has not been reported literatures. Sea clutter simulation using the cumulative distribution function (CDF) k is another novelty. Detection of moving target on sea surface with given curved path of the radar platform and real parameters for the simulation have also been performed for the first time.

Keywords: Radar, Monopulse, Grazing angle, Curved path, Clutter.

Submission date:28, 03, 2018

Acceptance date:13, 11, 2018

Corresponding author: MortezaKazerooni

Corresponding Author Address: Electrical and computer university Complex, Malek-Ashtar University of Technology, Lavizan, Tehran, Iran

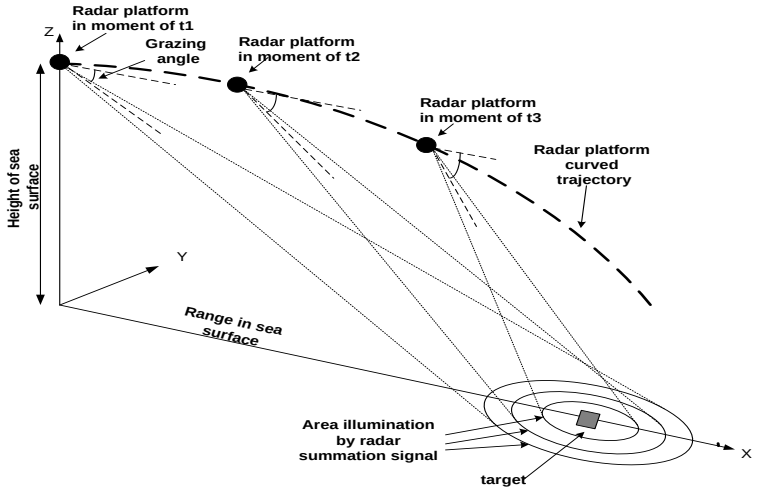

Fig. 1. Specifications and flight monopulse radar platform on a curved path

1. Introduction

Monopulse radar is used in guiding different platforms due to its high accuracy tracking. The tracking of sea targets is very important due to the sea clutter. When the grazing angle (the angle between the antenna and the horizon) of radar platform increases, the sea clutter becomes stronger and sea targets detection and subsequent tracking will be faced with an important challenge. So far not many articles have been published about this issue. The simulation of sea clutter is mostly done in PDF (probability distribution function) at constant height with very low grazing angles [1-16]. On the other hand, articles that have been published in the monopulse radar issue are mainly in following categories: improve ground based them on pulse radar performance in angle estimation [17-19]; improve performance against electronic ware fare measures [20,21]; SAR-monopulse radars and surface targets detection by the monopulse radar at fixed altitude and low grazing angle (less than 45 degrees)[22,23].

In this paper, array monopulse radar with uniform aperture illumination and maximum squint angle is considered. This radar is mounted on a platform with curved path (grazing angle of 55 to 75 degrees) and detects and tracks a large-scale floated target on the sea surface. The overview of the scenario is presented in Figure 1.

Due to the significant changes in the simulation parameters of sea Clutter at the angles studied in this paper (gamma function and Omega parameter), The novelty of this paper is simulation of the sea clutter in range and in high grazing angle (55 to 75 degrees), which has not been accomplished in published articles. Sea clutter simulation using the cumulative distribution function (CDF) k is another novelty of this paper. Detection of moving target on sea surface with given curved path of the radar platform and real parameters for the simulation have also been performed for the first time.

In this paper after the introduction, monopulse radar with the related equations for tracking and angular error is investigated in the second chapter. It the third chapter, sea clutter is expressed with respect to the direction of platform motion and equations and also corresponding distributions on range and cross range is investigated. By considering the changing of thegrazing angle, target detection height changes. In addition, due to the impossibility of monopulse radar segmentation in cross range, it is not possible to simulate sea clutter. Thus using different distributions in cross range, the target detection in this direction is done through processing techniques. However, to simulate sea clutter in range, given the k distribution characteristics such as the ability to create spatial-temporal correlation between the return signal data, enabling the use in situations with low probability of detection and high probability of false alarm, as well as compare it with the studies conducted on an experimental basis, it is selected as the closest mode to sea clutter in range and the corresponding relations and equations are discussed. In the fourth chapter, with regard to conditions considered, the sea clutter in the range is simulated based on parameters and the related results are deduced.

2. Mono-pulse Radar Angular Error Curve

It is assumed that the airborne radar antenna is an array with 20 elements in rows and columns that is uniformly

illuminated. The antenna produces two beams with maximum squint angle. Squint angle is the angle between the axes of the primary beams generated in the receiver and as this angle increases, monopulse radar angle coverage will increase in the parameters of the receiving antenna without altering. The maximum squint angle between the two primary beams is0.65of half-power beam width in range and cross range [24]

By dividing the difference voltage by the summation voltage, a curve based on the angular deviation from the axis of the antenna is formed which is known as the mono-pulse curve [25]. The angular error curve for 6 degrees half power beam width is shown in Figure 2. It should be noted that in Figure 2, the vertical axis is the ratio of difference signal (diff) to summation signal (sum). Simulation parameters are shown in Table 1.

In ground-based monopulse radar applications, the angular error curve measurement accuracy can be enhanced to some extent by forming an additional difference-difference channel, however, considering the 4 simultaneous channels and the occupied space, this method is not used in airborne monopulse radars [26]. It should be noted that noise interference in airborne monopulse radars using the domain comparison method, increases the angle finding error. Considering the Gaussian nature of this type of interferences, the methods for reducing or preventing these types of noises have been reported in the literature [27].

Table. 1. Specification of radar and radar carrier platform

Frequency	10 GHz
Power	100 W
Target radar area	4000 m^2
Height	15 Km
platforms speed	3300 m/s
Time to reach the target	~ 4 s
Half power beam width in cross range	6 degrees
Half power beam width in range	6 degrees
Grazing angle	55 to 75 degrees
Average sea clutter speed	5 m/s
Target dimensions	60×60 m^2
Detection probability	0.6
False alarm probability	10^{-6}
Noise	3 dB
Attenuation	10 dB
Sea mode	3*

* Sea mode 3 is the closest to the general conditions of the sea.

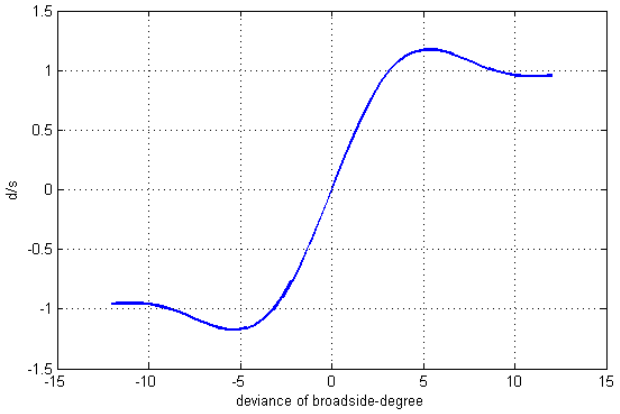

Fig. 2. Diagram for 6 degrees half power beamwidth angular error

3. Sea Clutter

One of the primary limitations in the performance of airborne radars and one of the main subjects in the development of radar guided platform speed design is the clutter presence. Illuminated Area on the sea surface by airborne radar is shown in Figure 3. Surface clutter in airborne radars is one of the important challenges in radar design, especially for target tracking on the surface or in low altitude over the surface. In addition to determining the frequency spectrum and radar pulse repetition frequency, this clutter has an effective role in determining the height of detection and tracking targets. In such radars, surface clutter is greater than the environmental noise level and in fact, the factor affecting the performance of the radar is the clutter. So, in equations used in radars, signal-to-clutter ratio (SCR) is used instead of signal to noise ratio (SNR).

3.1. Sea Clutter in Cross Range

In this case, target can be detected in cross range using range and Doppler gates or processing techniques such as frequency-Doppler space-time adaptive processing (STAP) and the tracking action can be carried out in cross range [28].

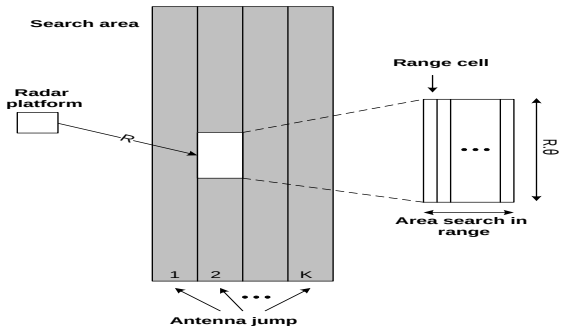

Fig. 3. Illuminated area on sea surface by airborne radar

3.2. Sea Clutter in Range

In the published articles so far in radar field, targets detection on the sea surface in low grazing angles (below 20 degrees) have been analyzed [3-7]. the important point in these articles is the existence of experimental model of sea clutter in the desired area which has been achieved by sending and receiving radar signals in that area.

Noting that the sea radar area is not uniform and is in fact random and also taking into account the characteristics of statistical models expressed in the published articles [3-12], the following is concluded:

1) The statistical results of numerous experiments show that k distribution provides a limited distribution of sea clutter.

2) k distribution is the best model to simulate sea clutter in areas that have a low probability of detection and false alarm.

3) With the exception of k distribution, other non-Rayleigh distributions are not derived from physical models or clutter reflectance methods and are only based on experimental results. These models are not able to provide time and space correlation data. To overcome this problem, k distribution is used because it has good accuracy in predicting the performance independent of correlation characteristics modeling accuracy compared to other domain distribution models.

Verification of this method for usual grazing angle to real radar sea clutter data is show in figure 4the data set used in this plot is taken from Farina et al [13]. The data from a single range cell. By visual inspection it can be noticed that amplitude distribution of the data best fit K distribution. Also, in Ward et al. [14]; Farina et al [15], the k distribution has been tested on several other data sets and has proven to be the distribution function of choice [16].

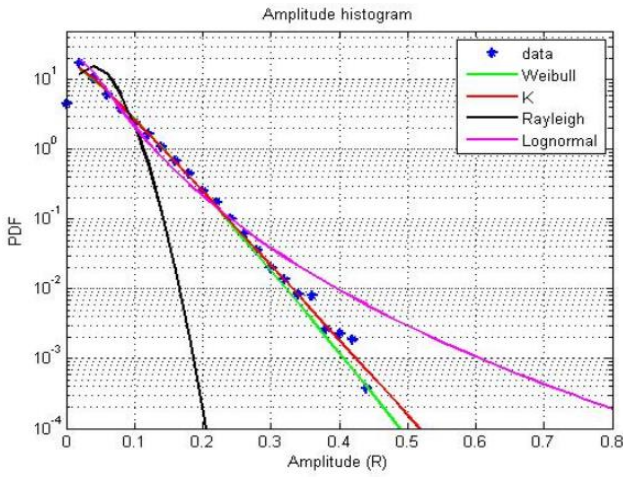

Fig.4. fitting non-Gaussian statistical distribution to real radar data Farina et al [13]

3.2.1. Clutter Model With k Distribution

K distribution model has a wide range of conditions and uses two parameters for modeling the returned sea clutter in high-resolution radars [3]. The first parameter is obtained by Chi distribution development and the second parameter is based on speckle pattern and Rayleigh domain distribution [2].

The first parameter indicates the slow changes and is associated with the sea surface large wave structures which are not altered by frequency agility. This parameter will be associated with the time correlation. The second parameter is associated with the rapid changes that show the interference between the small waves on the sea surface. This parameter becomes uncorrelated using frequency agility and its domain distribution corresponds to the pseudo-noise clutter.

In k distribution modeling, there are two important parameters: shape parameter υ and scale parameter c; the shape parameter determines the sea clutter sharpness. In fact, the smaller this parameter is, the sharper the sea clutter is. In practice, this parameter varies from 1.0 to 20 [2].

Scale parameter determines the power characteristic of return signals. The smaller the value of this parameter is, the stronger the signals returning from the sea surface are. Shape and scale parameters are proportional and the relationship between them is [2]:

$$c = \sqrt{\frac{4\upsilon}{P_t G_t^2 \frac{\lambda^2 f^4}{(4\pi)^3 R^3}\left(\sigma^0 \theta_{3dB} \frac{c_l \tau}{2}\right)}} \qquad (1)$$

In the above equation, P_t is the transmitter power in watts, G_t is the transmitter gain, λ is the wavelength of the radar in meters, $f^4$is the two-way antenna pattern on the surface, R is the mean distance from the clutter cells in meters, $\theta_{3dB}$is the antenna half power beam width in radians, τ is the pulse width in seconds, c_l is the speed of light in meters per seconds and $\sigma^0$is the mean clutter reflectance value or clutter radar area. The average

Amount of clutter reflectance changes with respect to the grazing angle is shown in Figure 5. This curve is deduced from the curve depicted in [11].

In order to simulate sea clutters using K distribution, we can use two distribution functions: PDF (probability distribution function) and CDF (cumulative distribution function). In the figure 6 two functions are plotted.

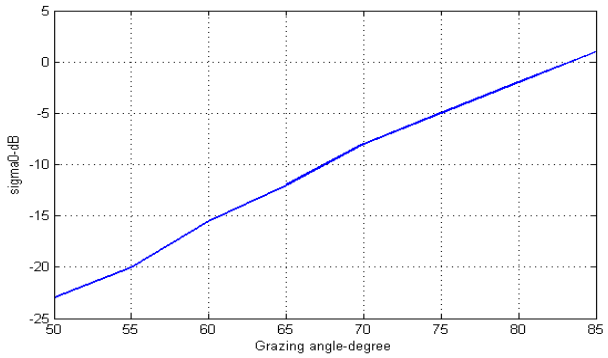

Fig. 5. Clutter radar area with respect to the grazing angle [29]

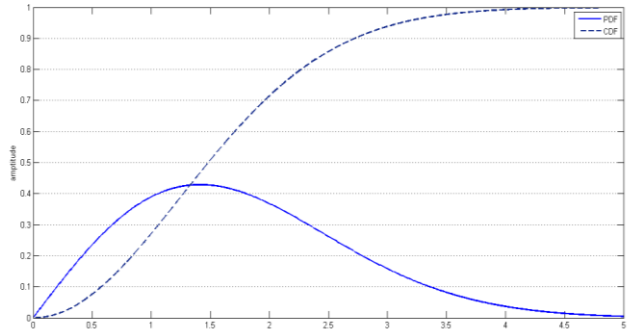

Fig.6. Comparison of PDF and CDF

As previously stated, PDF of K distribution is most similar form to the real sea clutter in low grazing angles. But at high grazing angles, the use of CDF is closer to real sea clutter values. The result is display in figure 7 for grazing angle of 70 degrees.

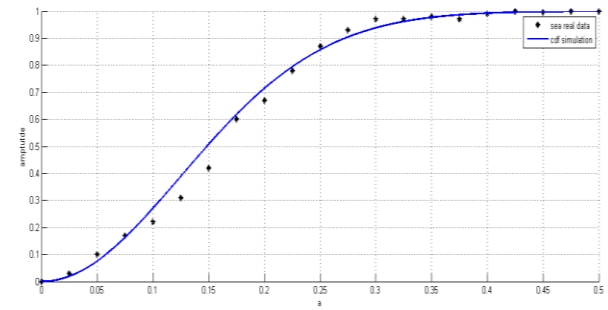

Fig.7.Fitting CDF of K distribution to real radar data Farina et al

In order to model the sea clutter, statistical distribution of sea radar area domain is obtained from the cumulative distribution function k. This function is given below [2]:

$$F_K(a) = 1 - \frac{2}{\Gamma(\upsilon)}(x)^{\upsilon}(\upsilon/\omega)^{\upsilon/2} K_{\upsilon}(a) \qquad (2)$$

In the above equation, υ is the shape parameter, ω is the omega parameter, K_υ is the modified Bessel function and Γ(υ) is the gamma function. "a" is a variable and is defined as follows [2]:

$$a = 2x\sqrt{\upsilon/\omega} \qquad (3)$$

In the above equation, x is a numerical variable greater than zero. The value of k function is shown in Figure 8. As shown in Figure 8, the slope of the curve and thus, the limits of reaching the amount of 1 (range of distribution curve k) is different at different grazing angles and this variation is of utmost importance in sea clutter simulation.

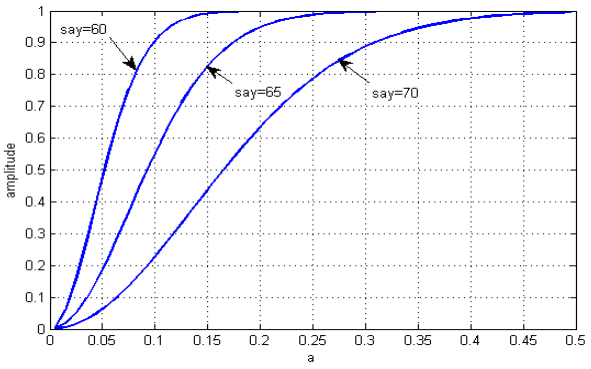

Fig.8. Cumulative distribution function k with respect to different grazing angles

By choosing random values from the distribution graph k (because of the randomness of reflection from the sea surface), sea radar area can be calculated by multiplying them with resolution in range and cross range (equal to half power beam width in cross range) and replace them in the clutter equation below [29].

$$C = \frac{P_t A_e \sigma^0 r_{range}}{(4\pi)^2 R^3} \qquad (4)$$

In the above equation, σ^o is the sea radar area, which varies according to the diagram shown in Figure 5with respect to the grazing angle. r_{range} is the radar range resolution in meters, P_t is the radar transmitter power in watts, A_e is the effective area of the antenna in square meters and R is the mean radar distance from the area illuminated by the main beam of the radar, in meters.

4. Simulation

In this chapter, three examples are investigated and simulated. These examples will be compared in the results in terms of clutter, signal and different grazing angles. It should be noted that the motion path and speed of radar platform in the three examples are considered and their parameters are given in Table 2. Simulation has been carried out using MATLAB software.

Table. 2. Simulation examples profiles

parameter	Example 1	Example 2	Example 3
Grazing angle (degree)	60	65	70
Half power beam width in cross range (degree)	6	6	6
Half power beam width in range (degree)	6	6	6
Altitude (meter)	15000	15000	15000
Target position in cross range (meter)	8500	7000	5600
Target position in range (meter)	500	500	500

In Table 2, thet arget position is located at the center of the main beam in range, approximately at the starting moment. Obviously, this situation will change with grazing angle and height of radar platform during the simulation. Range and cross range are the X and Y axis shown in Figure 1.

In the simulation, sea clutter in range is modeled with k distribution and signal and clutter in range is only shown in the diagrams. In Figures 9 to 11, the simulated graph of sea clutter (line) and the target signal (*) in 4 modes for 3 examples is presented.

Target and clutter signal processing during flying time until reaching the target is carried out in 88 moments. The amount of these moments is determined based on the intended processing method (which in this paper, I/Q processor is used taking into account two parameters of platform speed and the required accuracy) and the number of position data from the flight path. Considering the total time for tracking the target from the monopulse radar start moment until hitting the target (about 3.8 seconds), and taking into account the signal processing duration which is equivalent to 0.043 seconds, 88 processing moments (steps)occur in the tracking duration.

Considering the cycle amount of 2048 for FFT in processing (which is according to the number of data bits required in processing algorithms), and signal transmission to IF band with a frequency of 30 MHz, the summation and difference components are calculated in two channels of I and Q. By designing 5th order Butterworth filter with cutoff frequency of 300 MHz, the frequency response of the filter is calculated and k distribution of the clutter and homogeneous distribution is applied to range and cross range channels, respectively.

At this stage, applying filters on summation and difference channels in the two components of I and Q, the output of summation and difference in I and Q is calculated after taking FFT from the said values. Then, calculating d/s in two summation and difference channels, the closest angle to the target angle is calculated.

One advantage of I and Q processing is using synchronous detector (phase sensitive) which has a wider dynamic range than the envelope detectors used in the processing of linear range. Another advantage is the linear phase and domain(or logarithmic domain) processing capability in the spectral content of I and Q signals in the occupied IF bandwidth while processing domain or logarithmic domain and phase can be spread over a wider frequency band (4).

It should be noted that the grazing angle between 55 to 75 degrees condition holds in the simulation and to better display the charts, they are drawn based on moments 1, 15, 30 and 45. The results of the simulation are summarized in Table 3.

Obviously, the reason to select the three mentioned angles in Table 2 is the possibility of modifying the angle of the platform relative to the target. In fact, in example 1, selecting the initial 60 degrees grazing angle, it is possible to modify the grazing path to up to 75 degrees (about 15 degrees)with regards to the curved path that the platform traverses to reach the target (see Figure 1). However, in example 3, with selecting the initial grazing angle of 70 degrees, there is only 5 degrees of grazing angle modification by the platform so that the angle condition considered can be fulfilled.

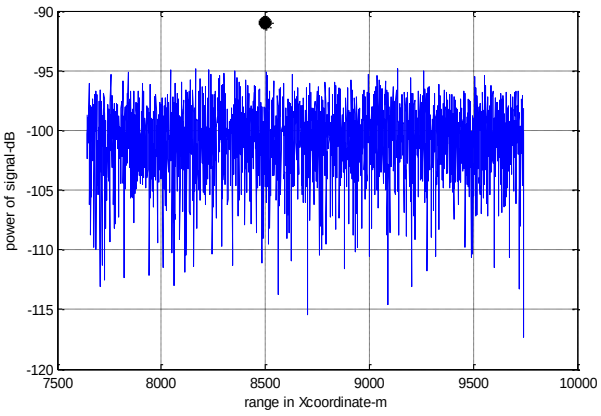

(a)

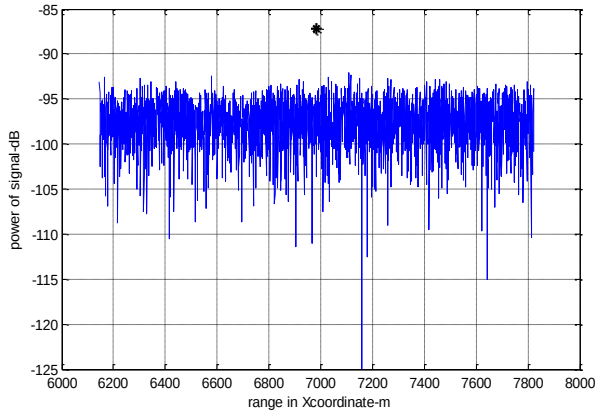

(b)

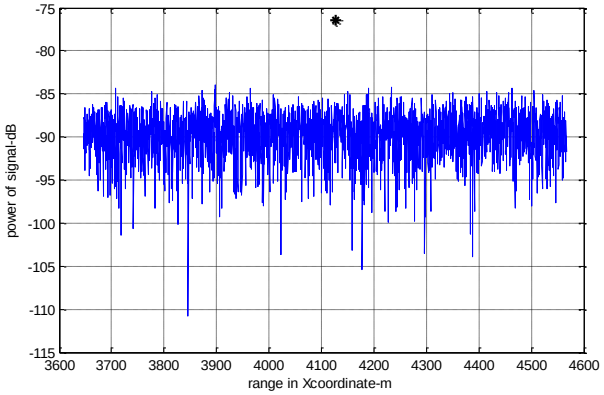

(c)

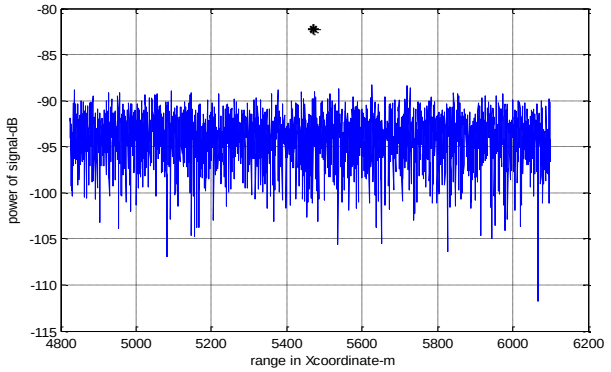

(d)

Fig.9. The results of the simulation of the signal and clutter for example 1;moment number 1 (a), moment number 15 (b), moment number 30 (c), moment number 45 (d)

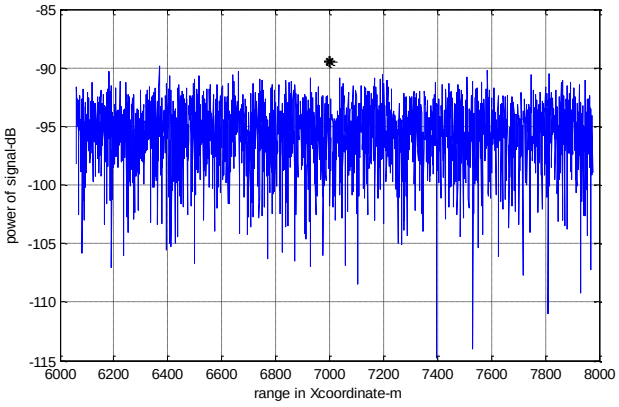

(a)

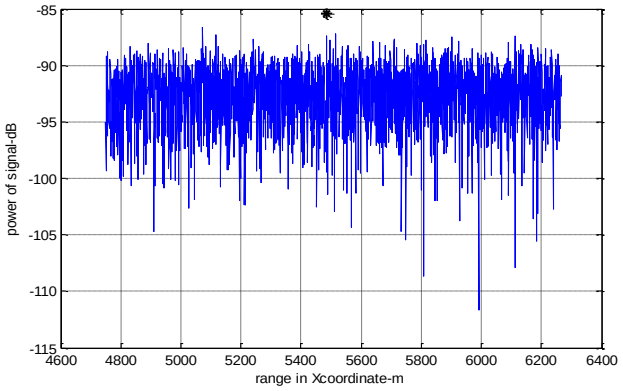

(b)

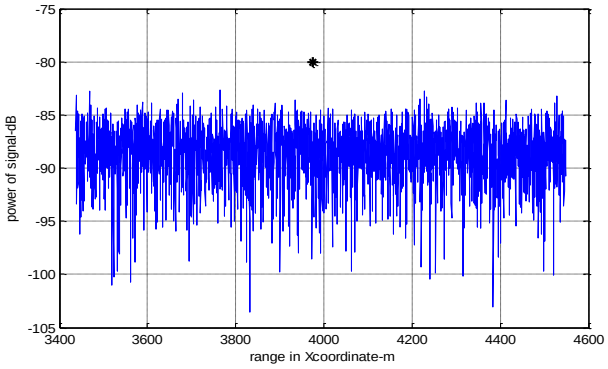

(c)

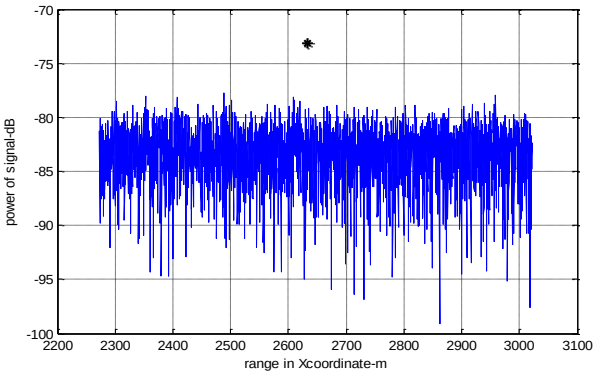

(d)

Fig.10.The results of the simulation of the signal and clutter for example 2; moment number 1 (a), moment number 15 (b), moment number 30 (c), moment number 45 (d)

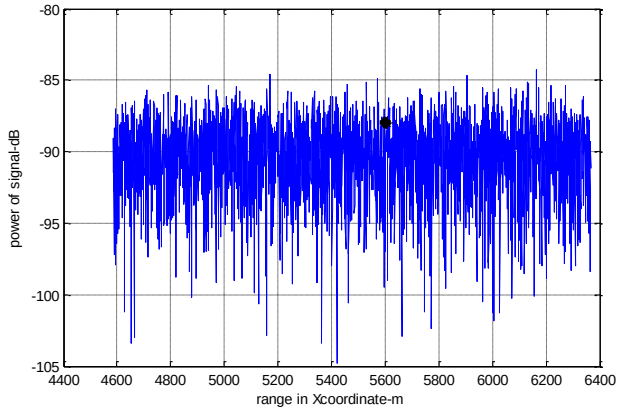

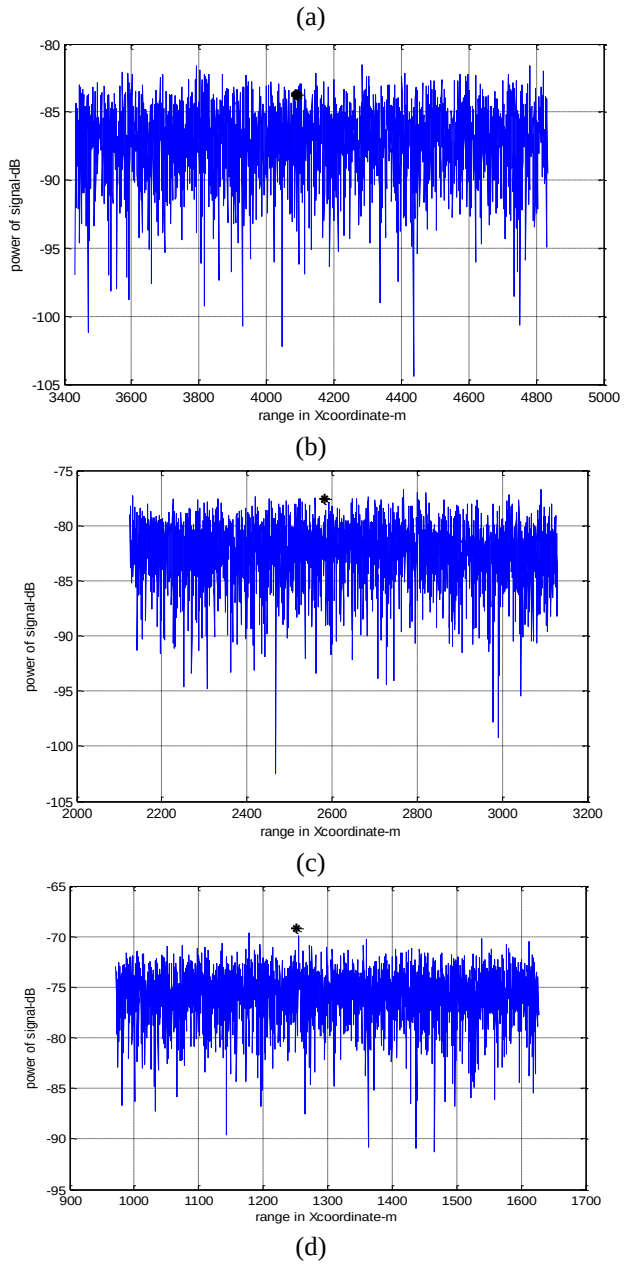

Fig.11.Results of simulation of signal and clutter for example 3; moment number 1 (a), moment number 15 (b), moment number 30 (c), moment number 45 (d)

Table. 3. Simulation Results

Altitude Of sea surface (m)	Example 1			Example 2			Example 3		
	S	C	|S-C|	S	C	|S-C|	S	C	|S-C|
14860	-92	-100	8	-89	-95	6	-87	-90	3
11932	-87	-97	10	-86	-93	7	-84	-87	3
8789	-82	-94	12	-80	-88	8	-77	-83	5
5969	-76	-89	13	-73	-83	10	-69	-76	7

S is the signal strength in terms of dB and C is the mean power of the clutter in terms of dB.

As it is shown in the simulation results in Table 3, detection height changes with respect to the grazing angle proportional to the level of detection threshold. Obviously, the lower is the detection threshold; detection takes place at higher altitude and also the possibility of false alarm increases and consequently, the detection probability decreases. The selection of an optimal threshold level requires a compromise between the cases presented.

Given the simulations carried out and considering the minimum threshold of 5 dB, the target detection height for the grazing angle of 60 degrees will be about 20 km, for the grazing angle of 65 degrees, about 15 km and for the grazing angle of 70 degrees, about 9 km.

As the values given in Table 3 demonstrate, with the constant half power beamwidth, increasing the grazing angle decreases the signal-to-clutter ratio. In fact, with increasing the grazing angle, the clutter signal strength will be much stronger than the return signal from the target, and while reducing the difference between the target and clutter signals, detection height will be reduced. In other words, in equal heights, the signal-to-clutter ration is inversely proportional to the increase in grazing angle.

5. Conclusion

Detection and tracking of sea targets is considered as one of the major challenges in airborne radar platforms due to the random structure of the sea surface and complexity of sea clutter, especially at high grazing angles. Using a proper distribution to simulate the sea surface so as to be very similar to the genuine return sea clutter will present a significant advantage in airborne radar design and processing algorithms. In this paper, using the cumulative distribution function k and taking into account the random feature of sea surface, sea clutter was simulated and taking into account the size of the target, the speed of the platform and the grazing angle, the signal detection height by airborne monopulse radarwith path motion was simulated and calculated. The results of the simulations carried out show that by increasing the grazing angle, the signal strength returning from the target decreases proportional to the clutter signal strength and therefore, the signal-to-clutter ratio and floated target detection height on the sea surface decreases.

References

[1]. L. Rosenberg, Sea-spike detection in high grazing angle X-band sea clutter, IEEE transactions on Geoscience and Remote sensing, Vol.51, No.8, pp 4556-4562, 2013.

[2]. Y. Dong, Clutter spatial distribution and new approaches of parameter estimation for weibull and K-distribution,

defense science and technology organization, Australia, 2004.
[3]. R. A. Paulus, Specification for a standard radar sea clutter model, scientific and technical information (STI) program of NASA, naval ocean systems center publication, san diago, 1990.
[4]. Taban M, Ghobadzadeh A, Hajimolahissieini H, Adaptive estimation of Clutter edge in Weibull Clutter using UMPI pre-detector, journal of Iranian association of Electrical and Electronics Engineers. 2012; 9 (1) :13-21.
[5]. I. Antipov, Simulation of sea clutter returns, electronic and surveillance research laboratory, Australia, 1998.
[6]. J. Hu, J. Gao, F. L. Posner, Y. Zheng, W. W. Tung, Target detection within sea clutter: a comparative study by fractal scaling analyses, World Scientific Publishing Company, Vol. 14, No.3, pp.187-204, 2006.
[7]. J. Carretero-Moya, J. Gismero-Menoyo, A. asensio-Lopez, A. Blanco-del-Campo, Small- target detection in sea clutter based on the radon transform, International conference on radar, Adelaide, AS, pp.610-615, 2008.
[8]. S. Panagopoulos, J. J. Soraghan, Small- target detection in sea clutter, IEEE transactions on geoscience and remote sensing, Vol.42, No.7, 2004.
[9]. F. Totir, E. Rador, L. Anton, C. Ioana, A. serbanescu, S. Stankovic, Advanced sea clutter models and their usefulness for target detection, MTA review, Vol. XVII, No.3, 2008, Vo;.18, No.3, pp.275-272.
[10]. A. Sinha, W. D. Blair, T. Kirubarajan, Y. Bar-Shalorn, Maximum likelihood angle extractor in the presence of sea-surface multipath, radar conference, pp.337-344, 2003.
[11]. V. T. Vakily, M. Vahedi, Sea clutter modeling improvement and target detection by Tsallis distribution, International conference on advanced computer control, singapor, pp.715-719, 2009.
[12]. A. Karimian, C. Yardim, W. S. Hodgkiss, A. E. Barrios, Multiple grazing angle sea clutter modeling, IEEE trasztion on antennas and propagation, Vol.60, No.9, pp.4408-4417, 2012.
[13]. W. J. Plant, A model for microwave Doppler sea return at high incidence angles: Bragg scattering from bound, tilted waves, Journal of geophusical research, Vol.102, No.C9,pp. 21131-21146, 1997.
[14]. A. Farina, F. Gini, M. Greco, and L. Verrazzani, High resolution sea clutter data: statistical analysis of recorded live data, in Radar, Sonar and Navigation, IEE Proceeding, vol. 144, pp. 121-130, June 1997.
[15]. K. D. Ward, R. J. A. Tough, and S. Watts, Sea Clutter: Scattering, the K distribution and Radar Performance. The institution of engineering and technology, 2006.
[16]. A. Farina, F. Gini, M. Greco, and L. Verrazzani, Analysis of sea clutter radar data, in Radar, 1996. Proceedings, CIE International Conference- of, pp. 115-118, October 1196.
[17]. T. O. Oyedokun, Sea Cutter Simulation, thesis for the degree of Master of Science in Engineering, Department of Electrical Engineering, University of Cape Town, May 2012.
[18]. Ghahramani H, Barari M, Suppressing strong sea Clutter based on DUET BSS, journal of Iranian association of Electrical and Electronics Engineers. 2015; 12 (2): 46-62.
[19]. L. L. Monte, R. Vela, L. Westbrook, Rediscovering monopulse radar with digital sum-difference beam forming, IEEE, Chicago, USA, July 2012.
[20]. S.A. Vashkevich, M. E. Fedorov, Raising the accuracy of a panoramic monopulse radar, IEEE measurement techniques, Vol. 46, No. 9,2003.
[21]. U. R. O. Nickel, Monopulse estimation with sub array output adaptive beam forming and low side lobe sum and difference beams, IEEE, Boston, USA, August 1996.
[22]. X. Yan, Y. Zhao, Q. Yang, P. Li, Research on synchronized non-coherent blinking jamming to monopulse radar seeker, IEEE, pp. 1753-1756, 2009.
[23]. B. Zhou, R. Li, L. Dai, H. Li, Combining sum-difference and auxiliary beam adaptive monopulse algorithm at sub array level for anti-jamming, IEEE international conference on signal processing, pp. 277-282, 2014.
[24]. M. Ruegg, M. Hagelen, E. Meier, D. Nuesh, Capabilities of dual- frequency millimeter wave SAR with monopulse processing for ground moving target indication, IEEE transaction on geoscience and remote sensing, Vol.45, No.3, pp. 539-553, Mar 2007.
[25]. M. Soumekh, Moving target detection and imaging using an X-band along-track monopulse-SAR, IEEE transaction an aerospace and electronic systems, Vol. 38, No. 1, pp. 315-333, Jan 2002.
[26]. Leonov. A. I, Fomichev. K. I, Monopulse Radar, Press: Artech House, 1986.
[27]. S. M. Sherman, D. K. Barton, Monopulse Principles and Techniques, 2nd edition, Artech House, Norwood, 2011
[28]. K. B. Yu, Enhanced monopulse angle Estimation using 4-channel radar system, IET International radar conference, Hangzhou, pp:1-6, 2015.
[29]. H. Paik, N. N. Sastry, I. Santiprabha, Effectiveness of Noise jamming white Gaussian Noise and phase Noise in Amplitude comparison monopulse radar receivers, IEEE international conference, Bangalore, pp 1-5, 2014.
[30]. M. Shen, J. Yu, D. Wu, D. Zhu, Space-Time adaptive monopulse for RD-STAP parameters estimation, IEEE China Summit and international conference, Chengdu, pp:283-287, 2015.
[31]. M. Skolnik, Introduction to Radar Systems, 3th edition, Tata McGraw-Hill Publishing, New Delhi, 2001.